Viscosity Measurements of Very Thin Polymer Films

Chunhua Li,[†] T. Koga,[†] C. Li,[†] J. Jiang,[†] S. Sharma,[†] S. Narayanan,[‡] L. B. Lurio,[§] X. Hu,[‡] X. Jiao,[‡] S. K. Sinha,[∥] S. Billet,[⊥] D. Sosnowik,[⊥] Hyunjung Kim,[#] J. C. Sokolov,[†] and M. H. Rafailovich*[,†]

Department of Materials Science and Engineering, State University of New York at Stony Brook, Stony Brook, New York 11794-2275; Advanced Photon Source, Argonne National Laboratory, Argonne, Illinois 60439; Department of Physics, Northern Illinois University, DeKalb, Illinois 60115; Departments of Physics, University of California San Diego, La Jolla, California 92093; Stella K. Abraham High School, Hewlett, New York 11557; and Department of Physics and Interdisciplinary Program of Integrated Biotechnology, Sogang University, Seoul 121-742, Korea

Received March 2, 2005; Revised Manuscript Received April 6, 2005

ABSTRACT: We have measured the viscosity of thin polymer films on Si substrates using three independent, yet complementary techniques: bilayer dewetting measurements where the viscosity of the lower layer is derived from the opening velocity of dewetting holes in the more viscous upper layer, X-ray photon correlation spectroscopy (XPCS) where the viscosity of a single layer is determined from the relaxation rate of thermally induced surface roughness, and dynamic secondary ion mass spectroscopy (DSIMS) where the viscosity is derived from measurements of the tracer diffusion coefficient. The scaling relationship, $\eta \sim M_{wPS}^{\alpha}$, yielded $\alpha = 3.3 \pm 0.3$ and $\alpha = 3.2 \pm 0.1$ from dewetting and XPCS measurement, respectively, which was in excellent agreement with the bulk scaling of 3.4 and the prediction from reptation theory. The absolute magnitudes were consistently higher by at most a factor of 3 than the bulk values, except for the sample studied at lower temperatures (155−170 °C) using XPCS. The temperature dependence in each case was weaker than the bulk values. These effects were interpreted in terms of attractive interactions with the Si surface which confined the polymer chains and affected the dynamics near the interface.

Introduction

In complex mechanical system, lubricants reduce friction and protect moving parts against wear. Ultrathin film lubricants are becoming increasingly important as miniaturization imposes increasingly tighter tolerances on devices ranging from microelectronics to biomedical components.

The efficiency of a lubricant depends on its viscosity and its ability to wet the surface. Unfortunately, viscosity measurements of polymer films thinner than a few microns are extremely difficult by standard methods since unphysical high shear rates are required to impose a measurable deformation over such small distances. Moreover, it has been shown that rheological properties of polymer thin films, unlike their bulk counterpart, very much depend on the film thickness and the surface upon which it is applied.[1−4] It is therefore important to design a viscometer in situ to measure the thin film viscosity at its required thickness and on the surface it is intended to coat.

A rather simple technique may be the observation of dewetting velocities of a probe layer from a viscous coating on a surface. In the process of dewetting, large forces can be exerted by unfavorable surface interactions to slide a probe layer across a lubricant-coated surface. If the friction energy is dissipated in the bottom layer, such as in plug flow, then a measure of the viscous drag of the bottom layer can be easily determined from which the viscosity can be calculated. This method is somewhat simpler than mechanically dragging a probe, such as an AFM tip, since we do not need to consider other factors that affect friction measurements such as the normal force, tip area, or the tip−surface interactions.

In this paper, we demonstrate that the dewetting velocity can be used to accurately determine the viscosity of a polymer coating on a surface. Considering a polymer bilayer film composed of two immiscible liquids, the dewetting behavior is controlled by the spreading parameter S

$$S = \gamma_B - (\gamma_A + \gamma_{AB}) \tag{1}$$

where γ_B and γ_A are surface tension of the bottom layer and top layer, respectively, and γ_{AB} is the interfacial tension between the two layers. When $S < 0$, the surface energy of the substrate is less than the sum of the surface energy of the upper layer and the polymer interface; dewetting will occur in order to expose the lower surface and minimize the interfacial area.

Brochard et al.[5] have calculated the dewetting dynamics and shown that the rate at which the holes grow will depend on the relative viscosity of layers A and B and the mechanism for energy dissipation. They defined two situations: "solid substrate" behavior and "liquid substrate" behavior.

If $\eta_B \gg \eta_A$, that is, the viscosity of the bottom layer is much higher than that of the top layer, the bottom layer behaves solidlike. In this case, all the energy is dissipated in the less viscous top layer, and the dewetting velocity is predicted to be a constant and given as

$$V = \frac{1}{12 \ln \sqrt{2}} \frac{\gamma_A}{\eta_A} \theta_e^3 \tag{2}$$

[†] State University of New York at Stony Brook.
[‡] Argonne National Laboratory.
[§] Northern Illinois University.
[∥] University of California San Diego.
[⊥] Stella K. Abraham High School.
[#] Sogang University.
* Corresponding author: e-mail mrafailovich@notes.cc.sunysb.edu.

10.1021/ma050440g CCC: $30.25
Published on Web 05/19/2005

Table 1. Characteristics of the Polymers Used in This Study[a]

polymer	M_w	M_w/M_n	source	thickness (Å)	bulk η[13,22] at 164 °C (N s/m^2)
PS	123K	≤1.08	Pressure Chemical	1350	5.9×10^4
PS	200K	≤1.06	Pressure Chemical	1340	3.1×10^5
PS	290K	≤1.06	Pressure Chemical	1360	1.1×10^6
PS	400K	≤1.06	Pressure Chemical	1350	3.3×10^6
PMMA	155K	≤1.10	Polymer Source	250	4.3×10^8

[a] Note: bulk data are from refs 13 and 22.

Here, θ_e is the equilibrium Young's contact angle, and ln is a logarithmic factor of order 10 which is due to a divergence of the dissipation in a wedge. Qu et al.[6] have verified the relationships for both the velocity and growth of the rim surrounding the holes in this "solid-like" substrate condition by studying the dewetting of PS on PMMA. The dewetting velocity was found to be a constant and scaled with the PS molecular weight as $N_{PS}^{-\alpha}$, where $\alpha = 3.9 \pm 0.6$.

For the opposite case of a highly viscous liquid dewetting from a less viscous substrate, the flow in the rim is a plug flow and most of the energy is dissipated by the drag forces in the "liquid" substrate. This situation can be further divided into two cases, depending on the thickness of the bottom layer. In the case of a "bulklike" thick bottom layer, the dewetting velocity is predicted to be a constant and is given by

$$V = \frac{|S|}{\eta_B} \tag{3}$$

If the bottom layer is very thin, or the substrate is smooth so that the polymer melt slips at the substrate interface, the dewetting velocity is predicted to decrease with increasing time, and the diameter of the hole is expected to grow as $t^{2/3}$:

$$R = \left(\frac{\gamma^2 L^2 \theta_e}{\eta_B{}^2 e}\right)^{1/3} t^{2/3} \tag{4a}$$

where

$$\frac{1}{\gamma} = \frac{1}{\gamma_A} + \frac{1}{\gamma_{AB}} \tag{4b}$$

Here, L and e are the thickness of the B and A layers, respectively, and γ is an effective surface tension. θ_e is the equilibrium contact angle in Neuman construction. In both situations of eq 3 and 4, we therefore find that the dewetting velocity is related only to the viscosity of the bottom layer, in a well-defined manner. Hence, we can use this bilayer geometry and either eq 3 or 4 to measure the viscosity of the layer adjacent to the substrate. Since the viscosity is known to be a sensitive function of the interaction between the lubricant layers and the substrate, this technique potentially allows us to obtain accurate in situ measurements of very thin films, which are not possible with standard rheometers.

To evaluate the technique of dewetting viscometry, we also compared the results with those from other complementary techniques performed on the same samples. We used X-ray photon correlation spectroscopy (XPCS) to measure the relaxation rate of thermally induced surface roughness from which one can obtain the viscosity using the theory of capillary waves. Dynamic secondary ion mass spectroscopy (DSIMS) was used to measure the tracer diffusion coefficients which are related to the zero shear viscosity by the Einstein relation.

Experimental Section

Bilayer Dewetting. Commercially available monodisperse polystyrene (PS) and poly(methyl methacrylate) (PMMA) of various molecular weights were used in this study. The substrates in all cases were silicon wafers, with (1 0 0) orientation. Details regarding the polymer used are tabulated in Table 1.

The samples were prepared as follows: PS layers of various molecular weights were spun-cast from toluene solution onto HF etched Si wafers and annealed at 160 °C in a vacuum of 10^{-7} Torr to remove the residual solvent. The thickness of the layers was measured using ellipsometry and found to be around 1350 Å thick. PMMA thin films (M_w = 155K, approximately 250 Å thick) were spun-cast onto microscope glass slides and floated from deionized water onto the PS substrates. The bilayer sample represents melt property since the solvent evaporates during the spinning process. From Table 1, we can see that all the samples were designed such that $\eta_{PMMA} \gg \eta_{PS}$, where PMMA and PS refer to the "probe" and "test" layers, respectively. Figure 1 shows the schematic of the geometry of the sample.

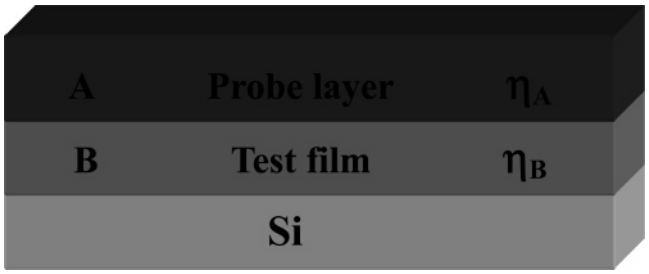

Figure 1. Schematic of the sample geometry. A liquid polymer layer B is spun-cast directly onto silicon wafer. A more viscous layer, A, is floated on top of the bottom layer.

After preparation, the films were allowed to dry before annealing at room temperature. The samples were then annealed at temperatures ranging from 150 to 180 °C in a high-vacuum oven (10^{-7} Torr). The oven was equipped with a specially designed load lock system which enabled us to anneal for short times and accurately determine the temperature. The samples were then quenched to room temperature, and the diameter of the dewetting hole was measured using an Olympus optical microscope. The time for each annealing was chosen to be 45 min, which is long enough to ignore the time of quenching and annealing the films to reach the desire temperature. A sign was made on each sample so that the same area could be observed after each anneal. The morphology of the holes was also measured using a Dimension 3000 SPM with a silicon nitride tip, in the contact mode.

X-ray Photon Correlation Spectroscopy (XPCS). Polystyrene (PS) films (approximately 1200 Å thick) were spun-cast on to HF etched Si wafers and annealed in a vacuum, as previously described. The XPCS experiments were performed at beamline 8-ID at the Advanced Photon Source (APS), Argonne National Laboratory. XPCS is a relatively new

technique which can be used to probe slow equilibrium dynamics. In equilibrium, the surface of a polymer film is roughened by thermally driven capillary waves. These random thermal features relax with characteristic time that depends on the film's viscosity. When a polymer film is illuminated with grazing incidence coherent X-rays, the surface roughness produces diffuse scattering, and the scattering pattern will fluctuate with a time scale determined by the relaxation rate of surface features whose wave vector matches the X-ray wavevector transfer. Specifically, the intensity−intensity time autocorrelation function, g_2, of the X-ray scattering pattern is proportional to the dynamic structure factor of the film, which can, in turn, be related to the viscosity of the polymer film using the theory of capillary waves. The off-specular diffuse scattering from PS thin film was recorded with a direct-illumination charge-coupled device (CCD) camera. The X-ray energy was 7.5 keV, and the incident angle was set to 0.15°, below the critical angle of 0.16°. Thus, the X-rays can only penetrate into the film to a depth of 100 Å, and the scattering from the Si substrate can be neglected. The beam dimensions were chosen to be 20×20 um^2, which was less than the X-ray coherence lengths. To avoid radiation damage, the sample exposure over the total correlation time was limited to less than 10 min. Details about this instrumental setup have been reported elsewhere.[7]

Dynamic Secondary Ion Mass Spectrometry (DSIMS). Monodisperse polystyrene (PS) and its deuterated analogues were used in this experiment. Hydrogenated PS films of molecular weight 200K (approximately 1270 Å thick) were spun-cast onto HF etched Si substrates and annealed at 160 °C to remove the solvent and relax residual stress. Another layer consisting of 15% 250K dPS and 85% 200K PS was spun-cast onto a clean glass slide and floated from deionized water onto the PS bottom layer to form a bilayer. The bilayer was annealed in a high vacuum oven (10^{-7} Torr), equipped with a load lock chamber maintained at a constant temperature preset at 150, 155, or 162 °C. The annealing times for each temperature were 3960, 1800, and 1200 s, respectively. The samples were then covered with a 300 Å thick sacrificial layer and analyzed. DSIMS was performed using an Atomika 3000-30 SIMS instrument by bombarding the sample with a 2 keV Ar ion beam at a 45° angle of incidence. The intensity of emitted ions (H^-, D^-, C^-, O^-, and Si^-) were measured as a function of time and used to convert the spectra into a concentration vs depth profile using the known film thickness. The setup of this instrument has been described in ref 8. The spatial resolution of this method was ≈80 Å.

Results and Discussion

Figure 2 shows typical optical micrographs of dewetting holes from a bilayer sample of a 155K PMMA (250 Å) film floated onto a Si substrate coated with a 123K PS (1350 Å) film. From the figure we see that the diameter of the holes increases with annealing time. To measure the viscosity of the PS layer, we focus on the region in the box shown in Figure 2 and measure the diameter of the holes as a function of time. Several of these areas were chosen across the sample, and the average diameter was obtained from 6 to 8 dewetting holes.

The microscopic details of the holes were also determined using atomic force microscopy (AFM). In principle, the contact angle can be obtained from the slope of the profile in the region close to the contact line. Figure 3a is the AFM cross-section image of the early stage of dewetting hole. From the image we see that the width of the rim was approximately 2 μm, and the dynamic apparent contact angle θ_A was observed to be $1.2 \pm 0.2°$. Figure 3b is the AFM cross-section image of the late stage of the dewetting pattern from which we obtained the equilibrium apparent contact angle θ_A ($1.5 \pm 0.2°$). In the classical Neuman construction, the equilibrium contact angle is given by $\theta_e = \theta_A + \theta_B$, where θ_A is the topographical apparent angle formed by liquid A and θ_B is the Neuman angle below the liquid/liquid interface. θ_A was obtained from AFM cross-section image as shown in Figure 3, and θ_B was calculated to be $27 \pm 4°$ through the Neuman equation ($\gamma_{A/B} \sin \theta_B = \gamma_B \sin \theta_A$).[9] Therefore, the equilibrium contact angle θ_e is known ($30 \pm 4°$).

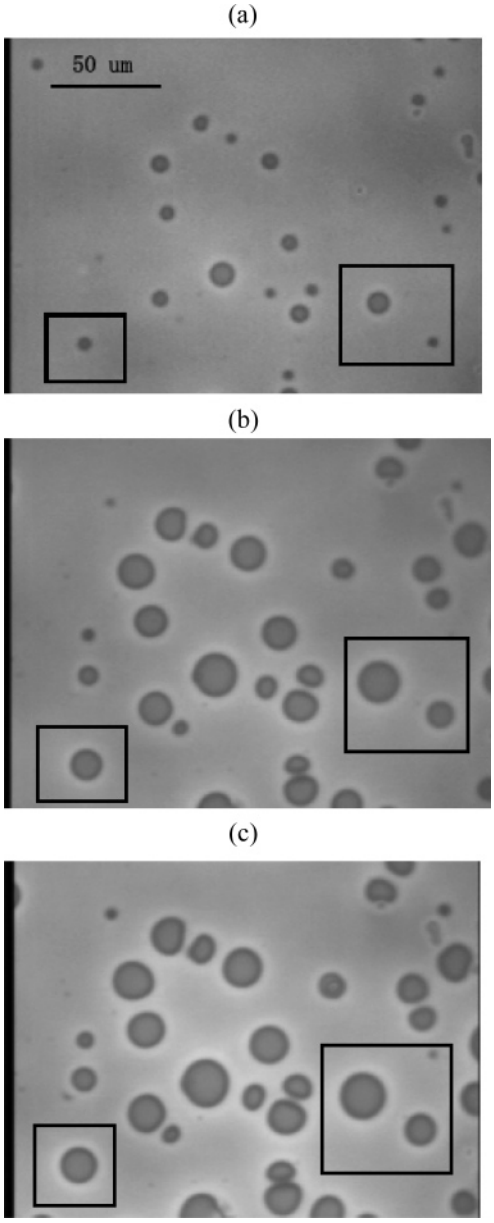

Figure 2. Optical micrographs showing holes due to a 155K PMMA (250 Å) film dewetting from a 123K PS (1350 Å) film after annealing at 164 °C for (a) 45, (b) 90, and (c) 135 min.

In Brochard's model,[5] the time-dependent scaling of the hole diameter will depend on the relative size of the film thickness and the width of the rim into which the material from the growing hole is collected. The diameter of the hole will grow linearly with time in the regime where the bottom layer thickness L is comparable to the lateral size, l, of the rim (eq 3), while a $t^{2/3}$ dependence is expected in the thin substrate regime where $L < l$ (eq 4a). In these experiments, the thickness of PS bottom layers was always approximately in the

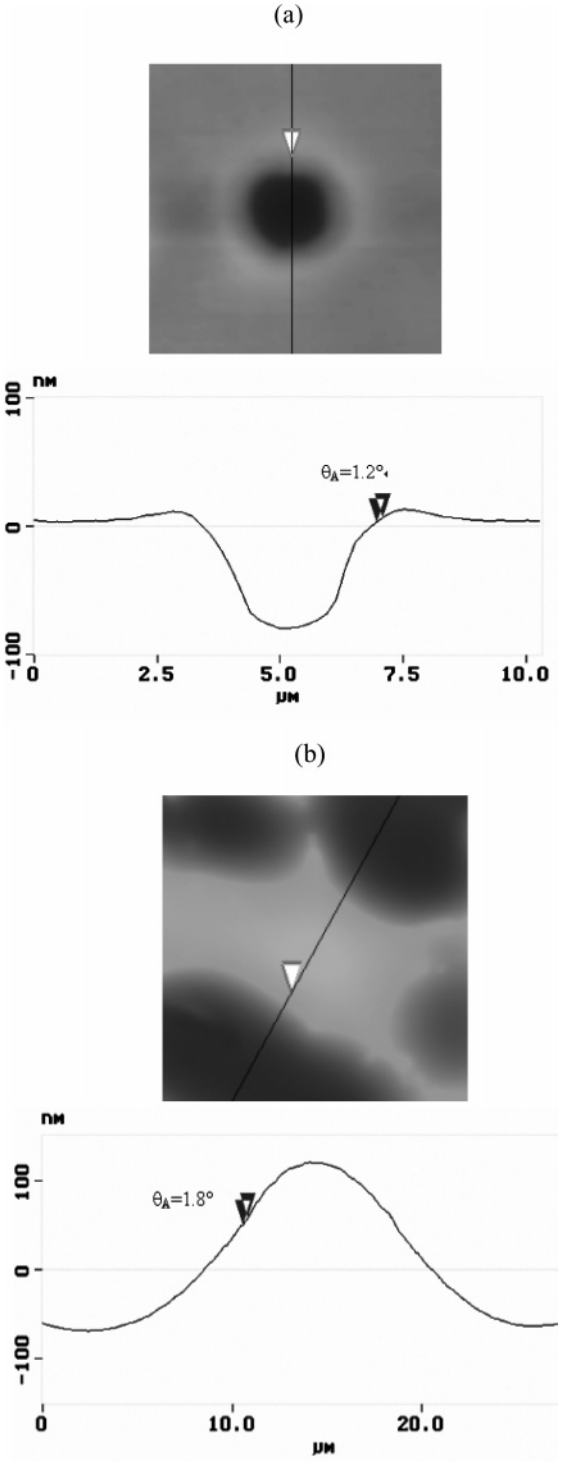

Figure 3. AFM cross-section image of a 155K PMMA (250 Å)/123K PS (1350 Å) bilayer film annealed at 175 °C for (a) 1 and (b) 24 h.

range of 1300−1400 Å while the rims, as can be seen from Figure 3, were approximately 2 μm wide, or $L/l \sim 6 \times 10^{-2}$ and all samples were well with the thin liquid substrate regime, described by eq 4a. The average diameter of the holes for films of different molecular weights is plotted as a function of annealing time in Figure 4a. From the figure we can see that the data, as expected, is well fit with a $t^{2/3}$ function (solid lines) for all the samples regardless of molecular weight. These results are in good agreement with Brochard's predictions[5] and previous results reported by Wang et al.[10] on thin PMMA liquid substrates of similar thickness.

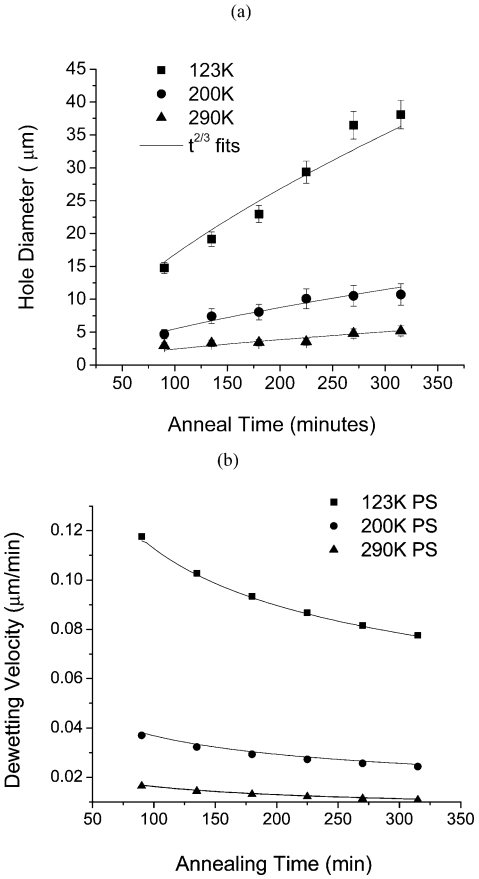

Figure 4. (a) Dewetting hole diameter as a function of annealing time for the samples of different molecular weights annealed at 164 °C. The solid lines are fits to eq 4a. (b) Dewetting velocities as a function of annealing time for the samples of different molecular weights; solid symbols represent the actual data annealed at different times.

The dewetting velocity can be obtained by differentiation of eq 4a:

$$V = \frac{\mathrm{d}R}{\mathrm{d}t} = \left(\frac{\gamma^2 L^2 \theta_e}{\eta_B{}^2 e}\right)^{1/3} t^{-1/3} \tag{4c}$$

In Figure 4b we plot the dewetting velocity as a function of annealing time according to eq 4c, where we see that the velocity decreases as more polymers accumulates into the rims.[5] The solid points shown in the figure correspond to the actual data for the samples annealed for different times.

We can now probe whether the agreement with theory is quantitative by comparing the viscosity derived from eq 4c with previously measured bulk values. Substituting the known values for γ_B, γ_A,[11] γ_{AB}[12] and the measured values for θ_e into eq 4c, we obtain the values of the viscosities plotted in Figure 5 as a function of molecular weight and in Figure 6 as a function of temperature. From the figures we can see that even though the values are within the same order of magnitude, the thin film viscosities are consistently higher by a factor of 2−3 than the bulk. As discussed previously in the literature,[1,2] this may be due to the attractive interactions between PS and the Si substrates which are known to decrease the chain dynamics near the interface.

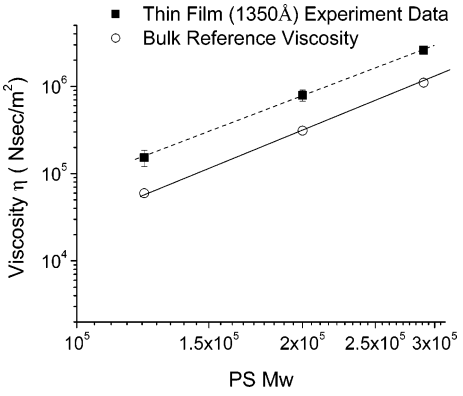

Figure 5. Log−log plot of the film viscosities derived from dewetting velocity as a function of PS molecular weight for films, approximately 1350 Å thick, annealed at 164 °C. The open symbols correspond to the bulk values.

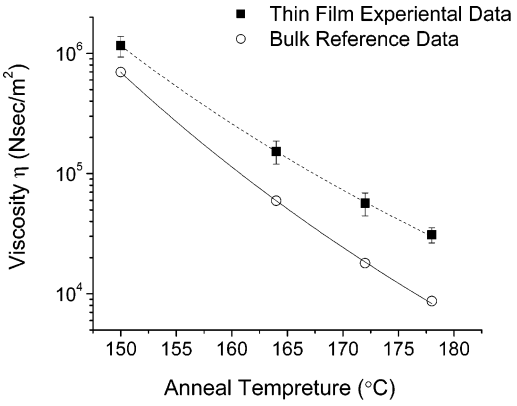

Figure 6. Thin film viscosity derived from dewetting measurements from a 155K PMMA (250 Å) film dewetting from a 123K PS (1350 Å) film annealed at temperatures ranging from 150 to 180 °C. The dashed and solid lines correspond to the fits to the WLF equation for the thin film and bulk values, respectively.

The scaling relationship of the viscosity as a function of molecular weight, $\eta \sim M_{wPS}^{\alpha}$, for thin films can be obtained from the slope of the double-logarithmic plot in Figure 5. The corresponding values obtained from the literature for bulk PS[13] at the same temperature are plotted as open symbols. From the data, we obtain $\alpha = 3.3 \pm 0.3$, which is in very good agreement with $\alpha = 3.4$ measured in the bulk[14] and the reptation theory.

The temperature scaling of the viscosity in thin films near surfaces can now also be determined. In Figure 6 we plot the viscosity obtained from eq 4c for PS films of $M_w = 123$K as a function of temperature. The dashed lines correspond to fits of the data with the Williams−Landel−Ferry (WLF) equation, where T_0 was chosen as 150° C

$$\log\left(\frac{\eta}{\eta_{T_0}}\right) = \frac{-C_1(T - T_0)}{C_2 + (T - T_0)} \tag{5}$$

The solid lines correspond to the WLF relationship calculated for a bulk PS[13] sample of the same molecular weight. From the figure we see that the temperature dependence of the thin film viscosity is weaker than that of the bulk. The fitting values obtained from least-squares fits to the data are $C_1 = 7.88$ and $C_2 = 111.3$, which compare favorably with the bulk value of $C_1 = 9.63$ and $C_2 = 112.1$. The WLF relationship represents

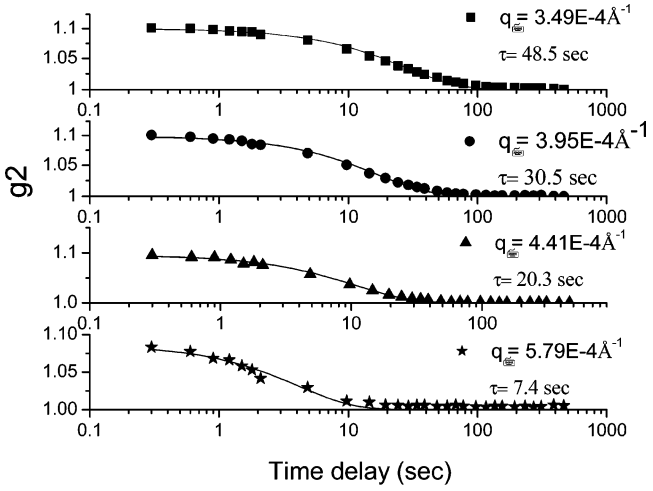

Figure 7. Autocorrelation functions obtained from XPCS at four different in-plane wave vectors measured for a 200K PS thin film (1150 Å thick) at 176 °C (symbols), compared with single-exponential fits (solid lines).

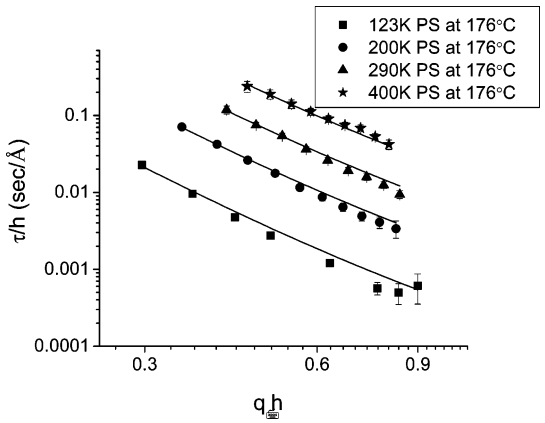

Figure 8. Relaxation time/film thickness vs in-plane wave vector × film thickness for PS thin films of different molecular weights 123K (squares), 200K (circles), 290K (triangles), and 400K PS (stars) annealed at 176 °C measured by XPCS. Solid lines are fits to eq 7.

an activated process with temperature. Desorption of the adsorbed moisture from the Si surface is also a temperature-activated process, which may add additional terms to the WLF relationship. An exact description of this process is difficult, since as was shown by Shin et al.,[3] the surface interactions are also temperature dependent in a manner which depends on the initial surface treatments.

To test the validity of deducing the viscosity of films on surfaces from the dewetting velocity, we also measured the viscosity using X-ray photon correlation spectroscopy (XPCS), which uses different principles to extract this result. XPCS measures the normalized intensity−intensity time autocorrelation function, $g_2(q,t)$

$$g_2(q,t) = \frac{\langle I(q,t')\, I(q,t+t')\rangle}{\langle I(q,t')\rangle^2} \tag{6}$$

where $I(q,t')$ refers to the scattering intensity at the in-plane wave vector transfer q and at time t'. The brackets $\langle\ \rangle$ refer to averages over time t', and t is the delay time. Figure 7 shows the autocorrelation functions obtained at four different in-plane wave vectors $q_{||}$ for a 200 K PS film measured at 176 °C. From the figure, it can be

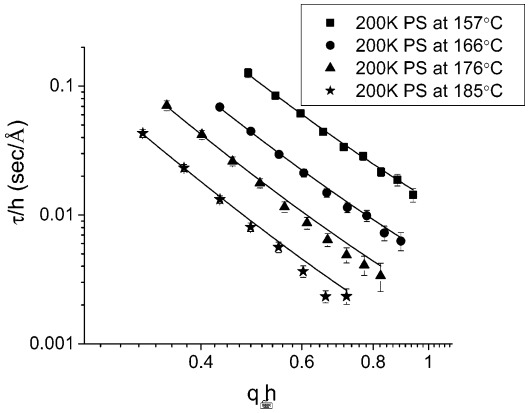

Figure 9. Relaxation time/film thickness vs in-plane wave vector × film thickness for a 200K PS film measured by XPCS at 157 (squares), 166 (circles), 176 (triangles), and 185 °C (stars). Solid lines are fits to eq 7.

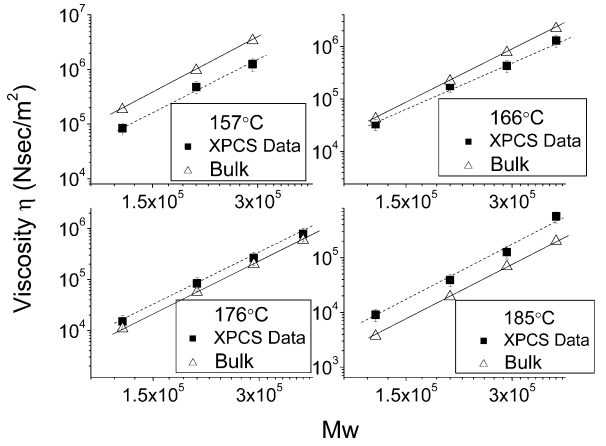

Figure 10. Thin film viscosities measured by XPCS and the corresponding bulk values[13] as a function of molecular weight.

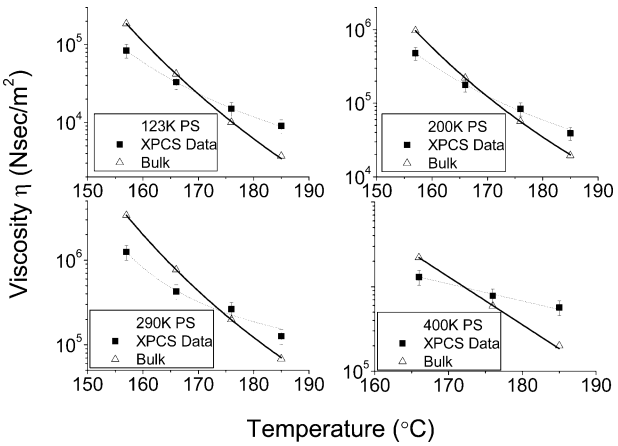

Figure 11. Thin film viscosities measured by XPCS and the corresponding bulk values[13] as a function of temperature for samples of different molecular weights. Solid lines and dashed lines are fits to the WLF equation for bulk and thin film data, respectively.

seen that the experimental data were well fit by an exponentially decaying autocorrelation function. The lines represent single-exponential fits, $g_2 = 1 + \beta \exp(-2t/\tau)$, where β is speckle contrast[7] and $\tau = \tau(q_{||})$ is the relaxation time for equilibrium surface height fluctuations.

On the basis of the theory of the dynamics of capillary waves on the thin viscous liquid films, Kim et al.[15]

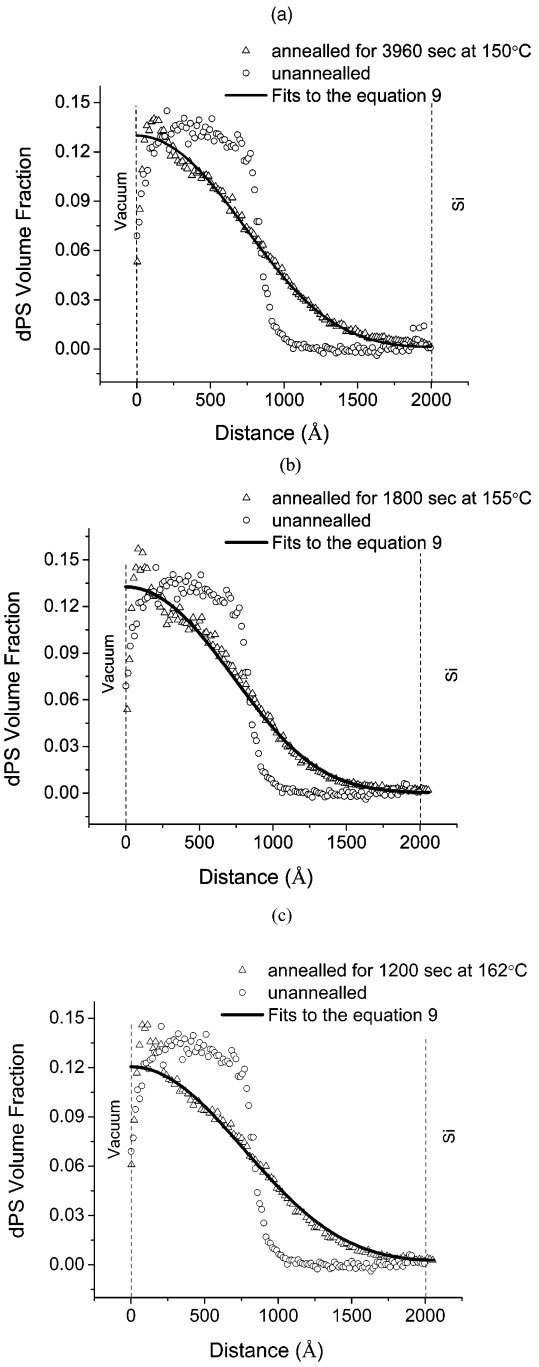

Figure 12. (a) DSIMS profiles of the deuterium concentration as a function of distance from the sample surface for the bilayer of 15% 250K dPS/200K hPS. Solid lines are fits to the Fickian equation (eq 9). Open circles correspond to the unannealed samples, and open triangles correspond to the samples annealed (a) at 150 °C for 3960 s, (b) at 155 °C for 1800 s, and (c) at 162 °C for 1200 s.

deduced the following expression for the relaxation time τ for capillary waves in the over damped region:

$$\tau \approx \frac{2\eta(\cosh^2(q_{||}h) + (q_{||}h)^2)}{\gamma q_{||}(\sinh(q_{||}h)\cosh(q_{||}h) - q_{||}h)} \tag{7}$$

where γ is the surface tension, $q_{||}$ is the in-plane wave vector, and h is the film thickness. Equation 7 indicates that τ/h should be solely a function of $q_{||}h$.[15,16] In Figure 8, we plot τ/h as a function of $q_{||}h$ for PS films of different molecular weights measured at 176 °C. Figure 9 shows

Table 2. Diffusion Coefficients Measured at Different Temperatures

top layer	bottom layer	annealing temp (°C)	annealing time (s)	diffusion coeff D ($\times 10^{-16}$ cm^2/s)
PS 200K + dPS 250K (15%) (730 Å)	PS 200 K (1270 Å)	150	3960	30
same	same	155	1800	60
same	same	162	1200	160

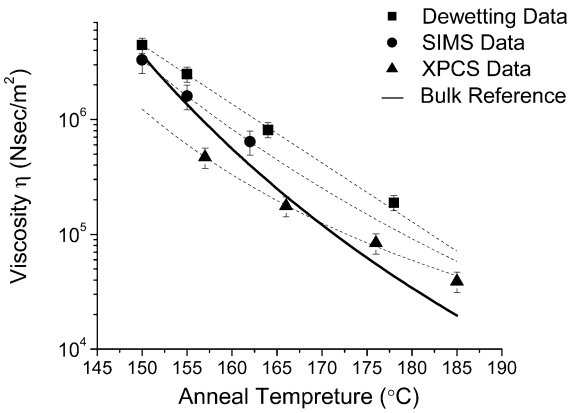

Figure 13. Comparison of the viscosity for PS films (M_w = 200K) measured by all three techniques, as a function of temperature. The dashed lines are fits to the data with the WLF relation (eq 5). The fit parameters for each curve are listed in Table 3.

τ/h as a function of $q_{||}h$ for a 200K PS film measured at different temperatures. From Figures 8 and 9, we observe that the relaxation time increases with increasing molecular weight and decreasing temperature. The solid lines in the figure are fits to eq 7. From eq 7 we see that τ/h is directly proportional to η/γ, and hence the viscosity of polymer thin film can be extracted from eq 7[15] using the measured surface tension of the polymer thin film reported by Lurio et al.[17]

In Figure 10, we plot, on a double-logarithmic scale, the viscosity (solid symbols) measured in situ at different temperatures as a function of the PS film molecular weight. For comparison, the corresponding bulk viscosity[13] is also plotted as open symbols. From the slopes of the linear fits in the scaling of $\eta \sim M_{wPS}^{\alpha}$, we find α = 3.2 ± 0.1, 3.0 ± 0.1, 3.3 ± 0.1, and 3.4 ± 0.1 at 157, 166, 176, and 185 °C, respectively. Hence, the scaling factor, as expected, is invariant with temperature and in good agreement with the bulk scaling and the prediction of the reptation theory.

From the figures we see that the viscosities measured by this method are again in agreement with the bulk values to less than an order of magnitude. On the other hand, the values seem to be smaller than the bulk at temperature below 170 °C, while at the temperature above 170 °C, the thin film values are greater than the bulk within the same range as those measured using the dewetting method. The temperature dependence of the film viscosity is summarized in Figure 11, where the solid and dashed lines are fits to WLF equation for bulk and thin films, respectively. From the figure we find that, in agreement with the dewetting results, the temperature dependence is weaker for the thin films on the solid substrates than in the bulk.

Measuring the tracer diffusion coefficient is yet another technique from which the viscosity of thin films can be deduced.[18] The diffusion coefficient is inversely related to the viscosity by the Einstein relation:

$$D = \frac{k_B T}{\eta_0 k_B / G(M) F(M,\upsilon)} \tag{8}$$

where η_0 refers to the zero shear viscosity. $G(M)$ depends on the entanglement molecular weight, and $F(M,\upsilon)$ is a function of the microstructural parameters of the polymer. From eq 8 we can derive the values of η_0 where $G(M)$ and $F(M,\upsilon)$ can be calculated from the data in Green et al.[18] The technique used to measure the concentration profiles, dynamic secondary ion mass spectroscopy (DSIMS), is different from the other two methods discussed previously and therefore provides another source of independent comparison.

Typical DSIMS data for unannealed and annealed samples are shown in Figure 12. Here we plot the concentration profiles of deuterium ions, which are proportional to the volume fraction of dPS, as a function of distance from the sample surface. The open circles correspond to the unannealed samples, while the open triangles correspond to the samples after annealing for 3960 s at 150 °C (Figure 12a), 1800 s at 155 °C (Figure 12b), and 1200 s at 162 °C (Figure 12c). The solid lines are fits to the Fickian equation[19,20]

$$\Phi(x) = 0.5\ \mathrm{erf}[(h - x)/\sqrt{4Dt}] + 0.5\ \mathrm{erf}[(h + x)/\sqrt{4Dt}] \tag{9}$$

where D refers to the tracer diffusion constant of the polymer chains, x is the distance from the sample surface, and h is the total sample thickness. The measured diffusion coefficients are summarized in Table 2.

The viscosity calculated from the Einstein relation (eq 8) is plotted as a function of temperature in Figure 13, together with the data obtained from the dewetting and XPCS measurements.[21] From the figure we find that, except for the sample studied at lower temperatures (155−170 °C) using XPCS, the viscosity in all cases is at most a factor of 3 higher than the bulk. The values obtained from DSIMS and dewetting are even closer or at most within a factor less than 2. The dashed lines in Figure 13 correspond to fits with the WLF relationship (eq 5), and the solid line represents the bulk values. The

Table 3. Rescaled Viscosities from Three Different Techniques

temp (°C)	η from dewetting (N s/m^2)	η from XPCS (N s/m^2)	η from SIMS (N s/m^2)	bulk η (N s/m^2)
150	$(4.5 \pm 0.5) \times 10^6$		$(3.3 \pm 0.5) \times 10^6$	3.6×10^6
155	$(2.5 \pm 0.3) \times 10^6$	$(6.8 \pm 1.0) \times 10^5$	$(1.6 \pm 0.2) \times 10^6$	1.3×10^6
165	$(8.1 \pm 0.5) \times 10^5$	$(2.0 \pm 0.3) \times 10^5$	$(4.6 \pm 0.7) \times 10^5$	2.6×10^5
175	$(1.9 \pm 0.3) \times 10^5$	$(1.0 \pm 0.2) \times 10^5$		6.6×10^4
185		$(3.9 \pm 0.5) \times 10^4$		1.9×10^4
WLF fitting parameter C_1	7.8	4.0	7.4	5.9
WLF fitting parameter C_2	143	62	113	63

WLF coefficients for each curve are also listed in Table 3 together with the viscosity values scaled with eq 5 so they can be directly compared. It can be seen that all the techniques show a consistent temperature-dependent behavior, where the change in viscosity is more gradual with temperature near the Si interface than in the bulk. The agreement between the techniques and with the bulk values indicate that all these methods provide good alternatives for in situ measurement of thin film viscosities on surfaces. Further experiments are currently in progress where we are probing these effects as a function of film thickness and surface interactions.[4]

Conclusion

We have measured the viscosity of thin polymer films on Si substrates using three independent, yet complementary techniques: bilayer dewetting measurements where the viscosity of the lower layer is derived from the opening velocity of dewetting holes in the more viscous upper layer, X-ray photon correlation spectroscopy (XPCS) where the viscosity of a single layer is determined from the relaxation rate of thermally induced surface roughness, and dynamic secondary ion mass spectroscopy (DSIMS) where the viscosity is derived from measurements of the tracer diffusion coefficient. The scaling relationship, $\eta \sim M_{wPS}^{\alpha}$, yielded $\alpha = 3.3 \pm 0.3$ and $\alpha = 3.2 \pm 0.1$ from dewetting and XPCS measurement, respectively, which was in excellent agreement with the bulk scaling of 3.4 and the prediction from reptation theory. The temperature scaling of the viscosity obtained from all three techniques was more gradual than the bulk. The absolute magnitudes were consistently higher than the bulk by at most a factor of 3 for annealing temperatures $T >$ 170 °C. In the temperature range of 155 °C $< T <$ 170 °C, DSIMS and dewetting data are in agreement with each other, and both are higher than the bulk values by approximately a factor of 2. The viscosity, measured by the XPCS method, on the other hand, is lower than the bulk in this regime by less than a factor of 2. The reasons for this discrepancy are not yet clear, but they may be due to the differences in preparation of the surfaces. Large changes in the oxide layer thickness were previously reported to occur in this temperature region which was postulated to affect the surface interactions with the polymer. Further work is in progress to determine the effects of surface interactions on the viscosity.

Acknowledgment. Support of this work by the NSF-MRSEC is gratefully acknowledged. H.K. acknowledges the support from the International Cooperation Research Program of the Ministry of Science and Technology of Korea (M6-0403-00-0079).

References and Notes

(1) Zheng, X.; Sauer, B. B.; Van Alsten, J. G.; Schwarz, S. A.; Rafailovich, M. H.; Sokolov, J.; Rubinstein, M. *Phys. Rev. Lett.* **1995**, *74*, 407.
(2) Zheng, X.; Rafailovich, M. H.; Sokolov, J.; Strzhemechny, Y; Schwarz, S. A.; Sauer, B. B.; Rubinstein, M. *Phys. Rev. Lett.* **1997**, *79*, 241.
(3) Shin, K.; Hu, X.; Zheng, X.; Rafailovich, M. H.; Sokolov, J.; Zaitsev, V.; Schwarz, S. A. *Macromolecules* **2001**, *34*, 4993.
(4) Li, C.; et al. Manuscript in preparation.
(5) Brochard-Wyart, F.; Martin, P.; Redon, C. *Langmuir* **1993**, *9*, 3682.
(6) Qu, S.; Clarke, C. J.; Liu, Y.; Rafailovich, M. H.; Sokolov, J.; Phelan, K. C.; Krausch, G. *Macromolecules* **1997**, *30*, 3640.
(7) Lumma, D.; Lurio, L. B.; Mochrie, S. G. J.; Sutton, M. *Rev. Sci. Instrum.* **2000**, *71*, 3274.
(8) Schwarz, S. A.; et al. *Mol. Phys.* **1992**, *76*, 937.
(9) Slep, D.; Asselta, J.; Rafailovich, M. H.; et al. *Langmuir* **2000**, *16*, 2369.
(10) Wang, C.; Krausch, G.; Geoghegan, M. *Langmuir*. **2001**, *17*, 6269.
(11) Brandrup, J.; Immergut, E. H.; et al. *Polymer Hand Book*, 2nd ed.; Wiley-Interscience: New York, 1989.
(12) Israels, R.; Jasnow, D.; Balazs, A. C.; Guo, L.; Krausch, G.; Sokolov, J.; Rafailovich, M. H. *J. Chem. Phys.* **1995**, *102*, 8149.
(13) Plazek, D. J.; O'Rourke, V. M. *J. Polym. Sci., Part A2* **1971**, *9*, 209.
(14) Doi, M.; Edwards, S. F. *The Theory of Polymer Dynamics*; Clarendon Press: Oxford, UK, 1986.
(15) Kim, H.; Rühm, A.; Lurio, L. B.; Basu, J. K.; Lal, J.; Lumma, D.; Mochrie, S. G. J.; Sinha, S. K. *Phys. Rev. Lett.* **2003**, *90*, 068302.
(16) Madsen, A.; Seydel, T.; Sprung, M.; et al. *Phys. Rev. Lett.* **2004**, *92*, 096104.
(17) Lurio, L. B.; Kim, H.; Rühm, A.; Basu, J. K.; Lal, J.; Sinha, S. K.; Mochrie, S. G. J. *Macromolecules* **2003**, *36*, 5704.
(18) Green, P. F.; Kramer, E. J. *J. Mater. Res.* **1986**, *1*, 202.
(19) Crank, J. *The Mathematics of Diffusion*, 2nd ed.; Oxford University Press: Oxford, England, 1975.
(20) Crank, J.; Park, G. S. *Diffusion in Polymers*; Academic Press: San Diego, CA, 1968.
(21) Note that the molecular weight of the dPS (250K) is slightly different than that of the hPS ($M_w = 200$K) used in the XPCS and dewetting measurements. Since the tracer diffusion corresponds to the viscosity of the dPS chains, the values plotted in Figure 13 were scaled by $(M_1/M_2)^{3.4} = \eta_1/\eta_2$ in order to be directly comparable.
(22) Fuchs, K.; Friedrich, C.; Weese, J. *Macromolecules* **1996**, *29*, 5893.

MA050440G